
Figures and figure supplements

A calibrated optogenetic toolbox of stable zebrafish opsin lines

Paride Antinucci *et al*

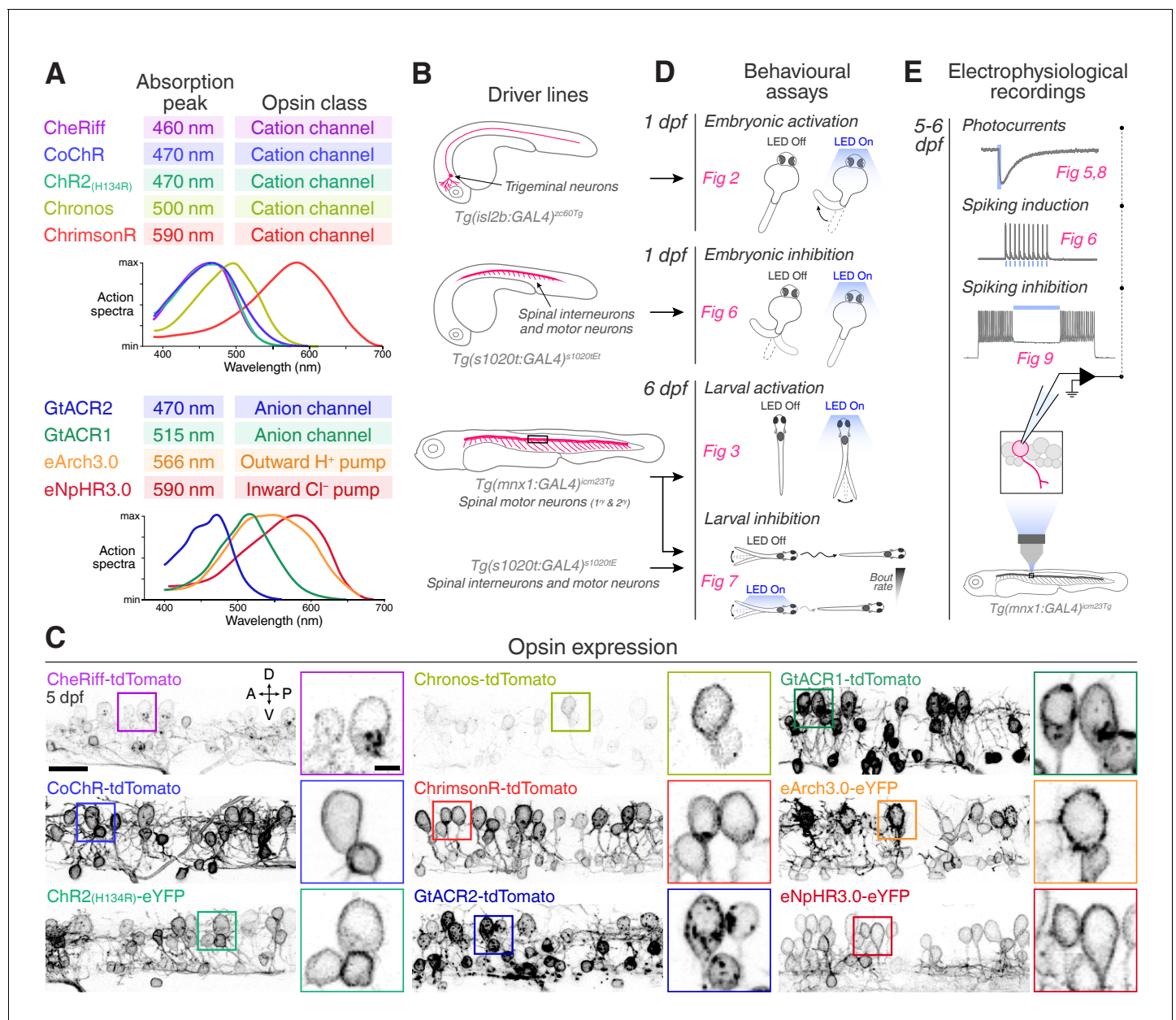


Figure 1. Toolkit for targeted opsin expression. (A) List of selected opsins, with spectral absorption and opsin class. (B) Schematics of expression patterns in the GAL4 transgenic driver lines used in this study. (C) Opsin expression in spinal neurons in *Tg(mnx1:GAL4;UAS:opsin-FP)* larvae at 5 dpf (for eNpHR3.0, the *s1020t:GAL4* transgene was used). Insets show magnified cell bodies to illustrate opsin membrane expression (for insets, brightness and contrast were adjusted independently for each opsin to aid visualisation). A, anterior; D, dorsal; P, posterior; V, ventral. Scale bar 20 μ m in large images, 5 μ m in insets. (D) Behavioural assays and corresponding figure numbers. (E) In vivo electrophysiological recordings and figure numbers. See also **Figure 1—figure supplement 1**.

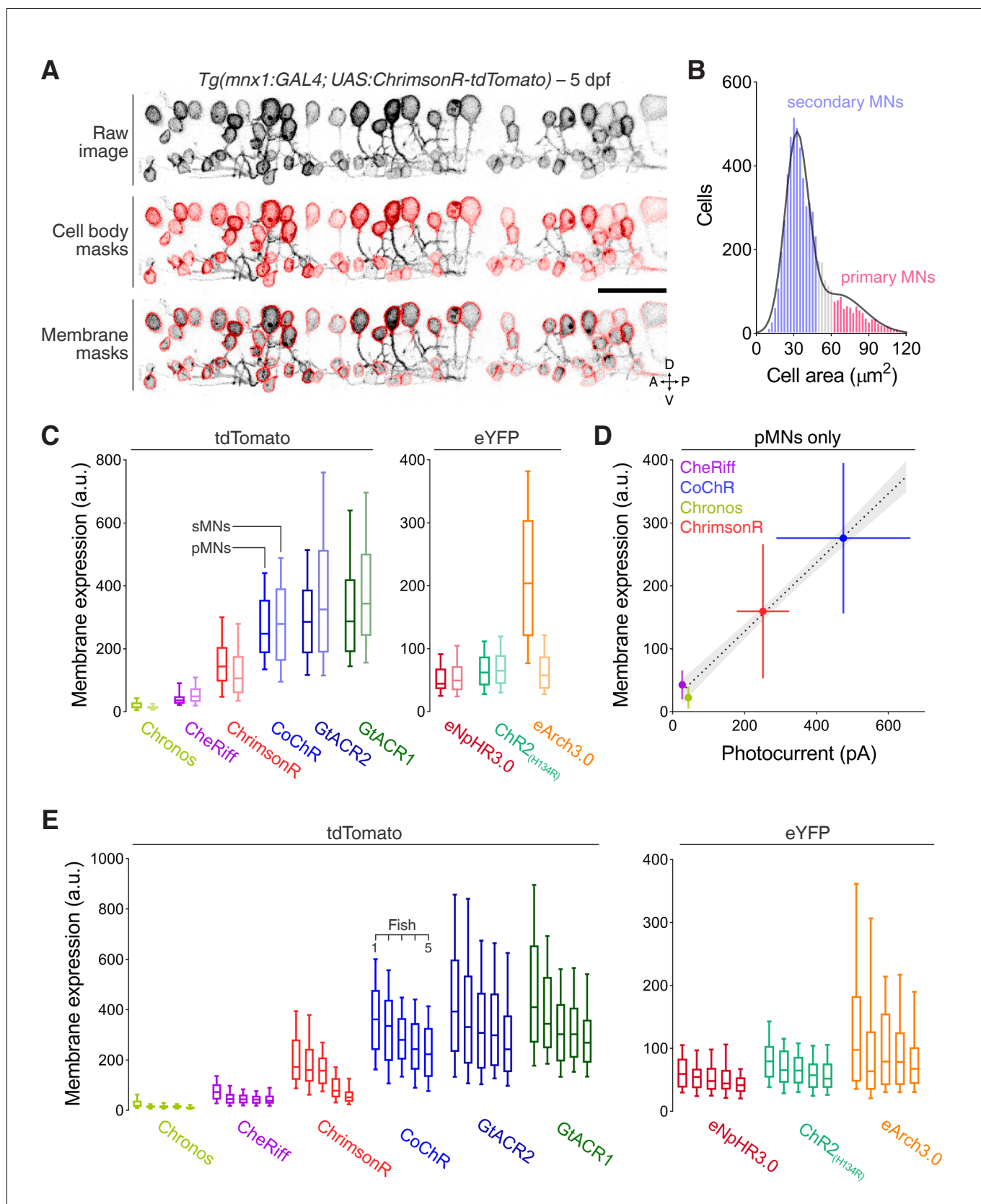


Figure 1—figure supplement 1. Analysis of opsin expression in larval motor neurons. (A) Opsin expression in spinal motor neurons in a *Tg(mnx1: GAL4;UAS:ChrimsonR-tdTomato)* larva at 5 dpf. Middle panel shows masks used to compute cell body area. Bottom panel shows masks used to Figure 1—figure supplement 1 continued on next page

Figure 1—figure supplement 1 continued

estimate membrane expression. A, anterior; D, dorsal; P, posterior; V, ventral. Scale bar 30 μm . (B) Cell body area and dorsoventral location in the spinal cord were used to classify cells as primary or secondary motor neurons (MNs) (**Menelaou and McLean, 2012**). Black line corresponds to sum of two Gaussians fit. Grey bars indicate unclassified neurons. (C) Opsin expression estimated as mean fluorescence intensity per membrane pixel in primary MNs (pMNs, dark) and secondary MNs (sMN, light). Opsins are grouped according to the fluorescent protein they are linked to. Box plots range from 10th to 90th percentiles. a. u., arbitrary units. (D) Opsin expression in pMNs vs. photocurrents in pMNs for cation channelrhodopsins linked to tdTomato. Error bars indicate standard deviation. Dotted line and grey areas correspond to linear fit with 95% confidence intervals. (E) Opsin expression across all neurons in individual fish (N = 5 larvae per opsin; Chronos, n = 302 cells; CheRiff, n = 998; ChrimsonR, n = 771; CoChR, n = 514; GtACR2, n = 1002; GtACR1, n = 735; eNpHR3.0, n = 386; Chr2_(H134R), n = 910; eArch3.0, n = 487).

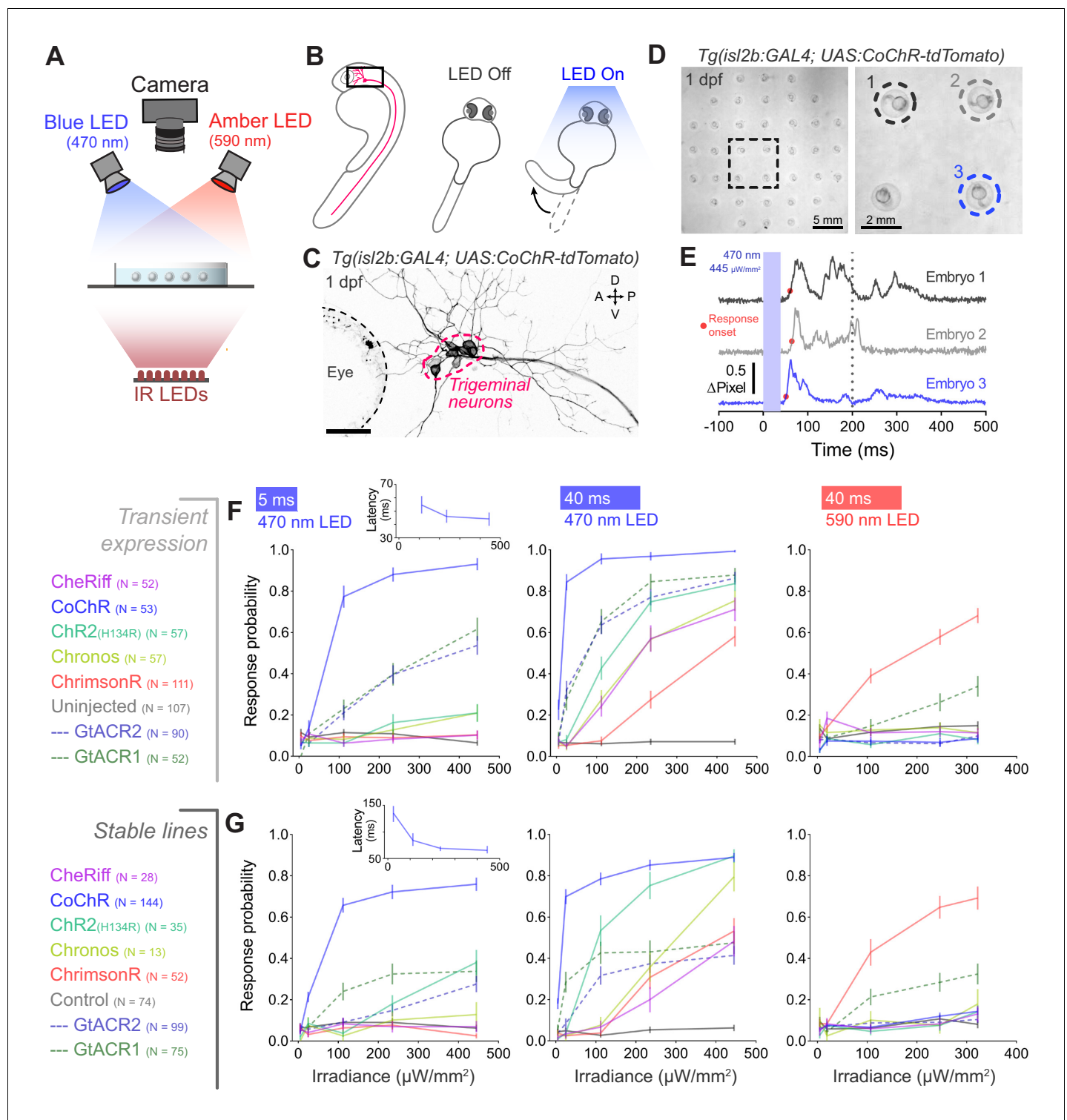


Figure 2. Optogenetic activation of embryonic trigeminal neurons triggers escape responses. (A) Experimental setup for optogenetic stimulation and behavioural monitoring. IR, infrared. (B) Schematic of behavioural assay. (C) Opsin expression in trigeminal neurons in a *Tg(isl2b:GAL4;UAS:CoChR-tdTomato)* embryo at 1 dpf. Imaging field of view corresponds to black box in (B). A, anterior; D, dorsal; P, posterior; V, ventral. Scale bar 50 μm . (D) *Tg(isl2b:GAL4;UAS:CoChR-tdTomato)* embryos positioned in individual agarose wells. Behaviour was monitored at 1000 frames per second across multiple embryos (28–30 hpf; N = 69 \pm 26 fish per opsin group, mean \pm SD) subjected to 5 or 40 ms pulses of full-field illumination (470 or 590 nm, 4.5–445 $\mu\text{W}/\text{mm}^2$) with a 15 s inter-stimulus interval. (E) Optogenetically-triggered escape responses detected from ΔPixel traces in the three embryos indicated in (D). Dotted line indicates maximum latency (200 ms) for a response to be considered optogenetically-triggered. (F,G) Response probability

Figure 2 continued on next page

Figure 2 continued

for transient (E) or stable (F) transgenic embryos expressing different opsins (mean \pm SEM, across fish). Insets show response latency for 5 ms blue light pulses in CoChR-expressing embryos (median \pm 95% CI, across fish). See also **Figure 2—figure supplements 1** and **2** and **Figure 2—video 1**.

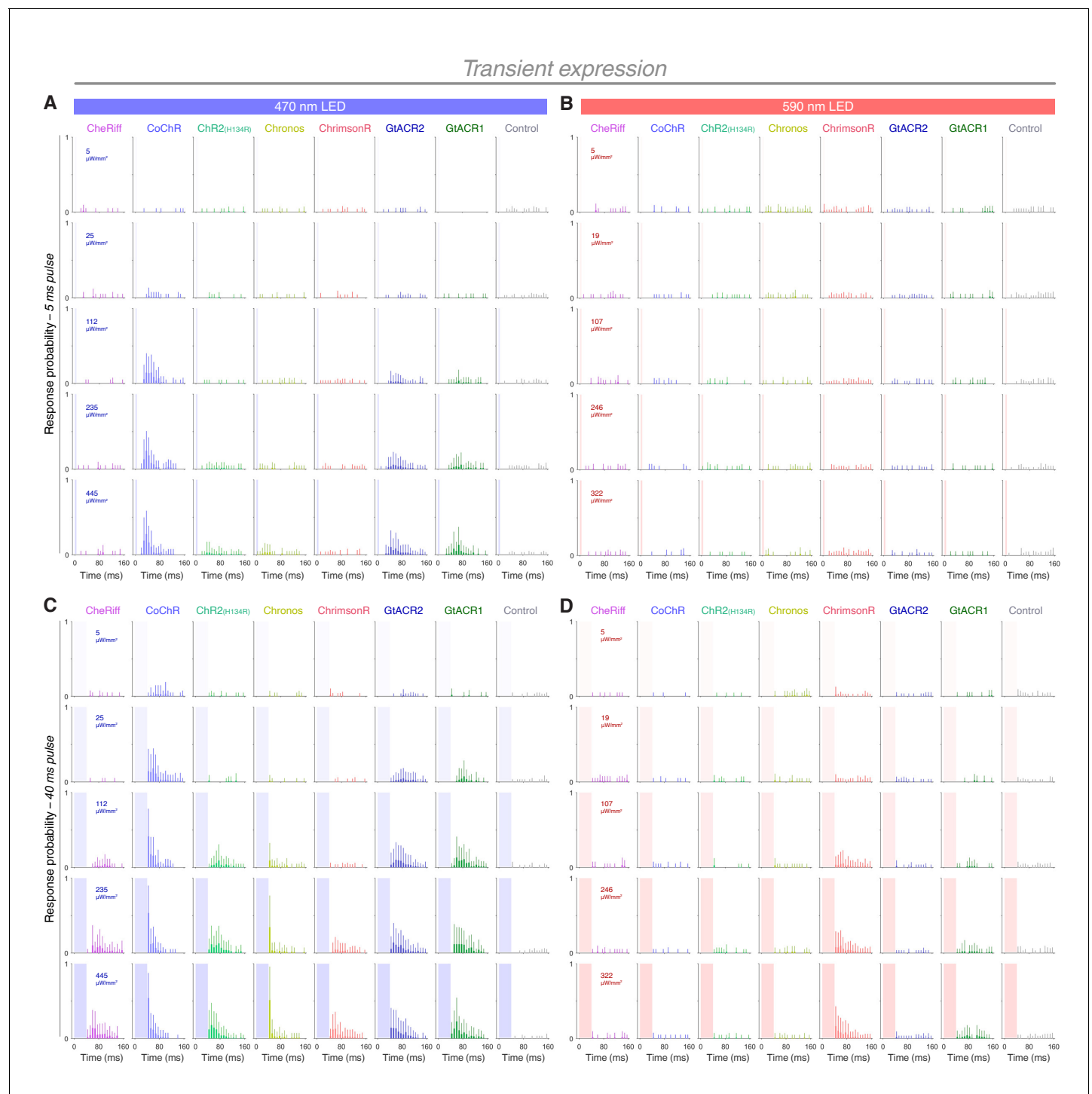


Figure 2—figure supplement 1. Response probability vs. time in transient transgenic embryos expressing opsins in trigeminal neurons. (A–D) Distribution of response probability vs. time for *Tg(isl2b:GAL4)* embryos (28–30 hpf) expressing different opsins through transient transgenesis (mean + SD, across fish). Embryos were stimulated with 5 ms (A,B) or 40 ms (C,D) pulses of blue (470 nm; A,C) or amber (590 nm; B,D) light. Each time bin corresponds to 8 ms.

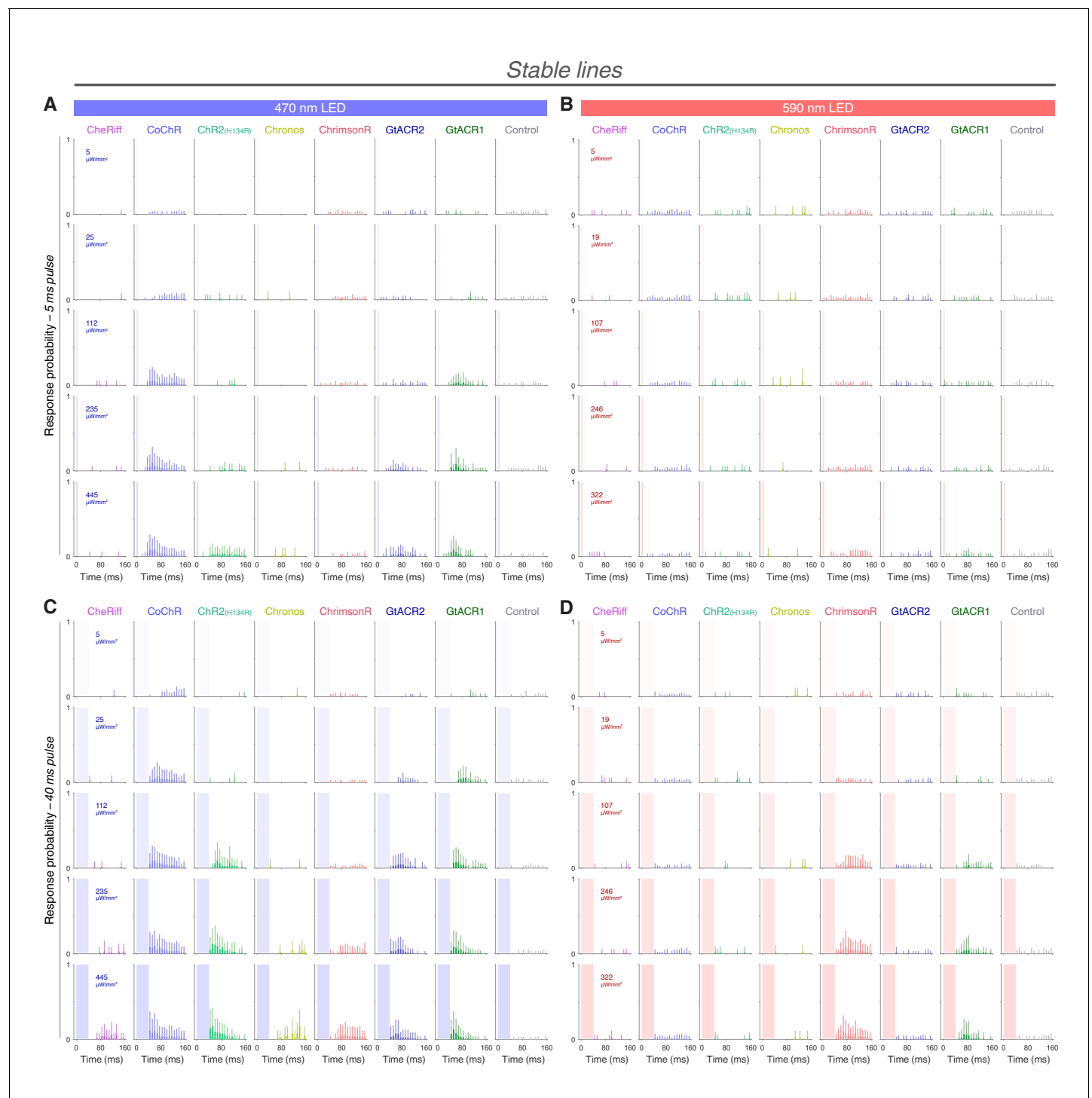


Figure 2—figure supplement 2. Response probability vs. time in stable transgenic embryos expressing opsins in trigeminal neurons. (A–D) Distribution of response probability vs. time for *Tg(isl2b:GAL4)* embryos (28–30 hpf) expressing different opsins through stable transgenesis (mean + SD, across fish). Embryos were stimulated with 5 ms (A,B) or 40 ms (C,D) pulses of blue (470 nm; A,C) or amber (590 nm; B,D) light. Each time bin corresponds to 8 ms.

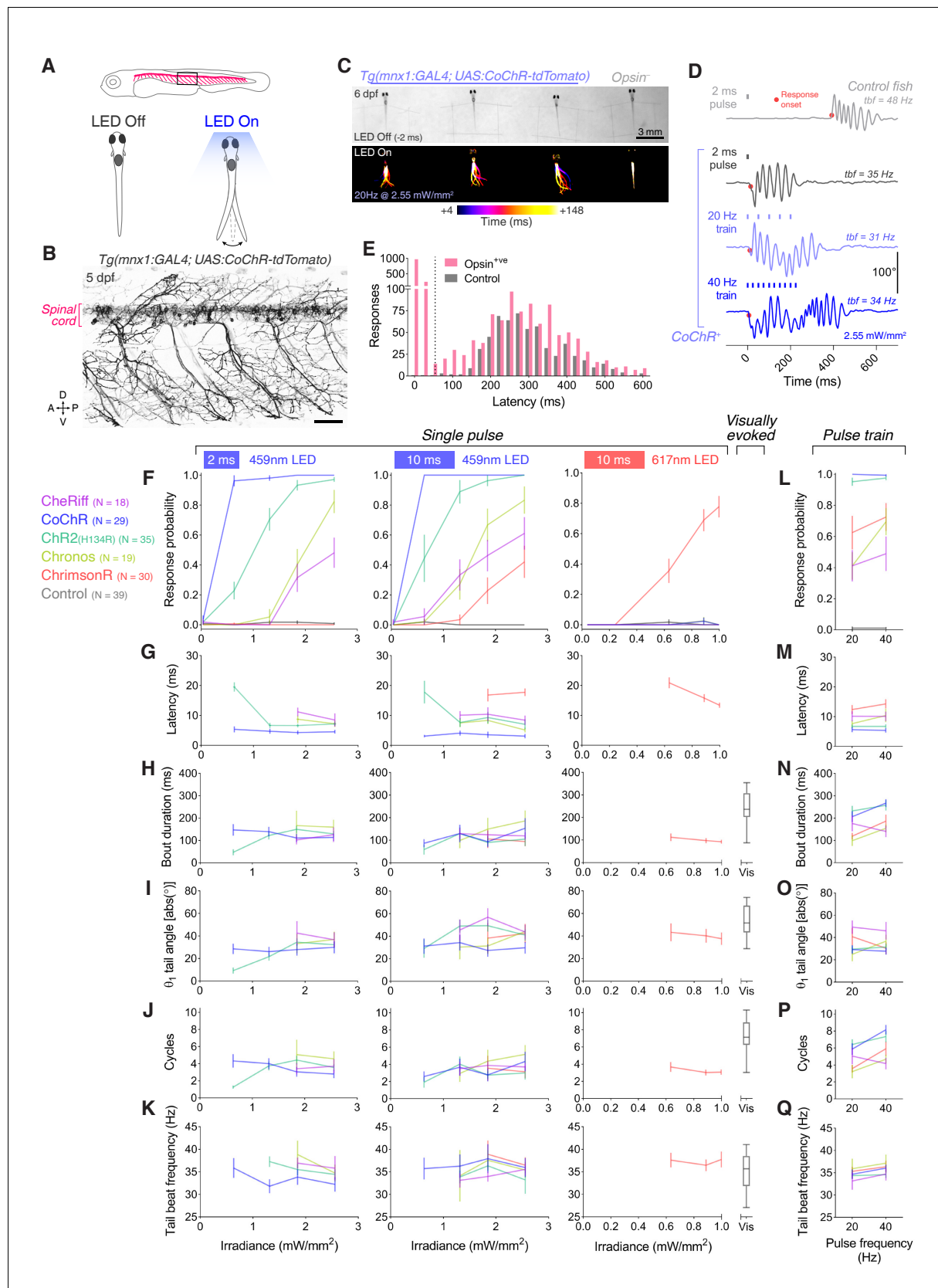


Figure 3. Optogenetic activation of larval spinal motor neurons triggers tail movements. (A) Schematics of behavioural assay. Head-restrained, tail-free larvae (6 dpf; N = 28 ± 8 fish per opsin group, mean ± SD) were exposed to 2 or 10 ms pulses of light (459 or 617 nm, 0.04–2.55 mW/mm²) with a 20 s Figure 3 continued on next page

Figure 3 continued

inter-stimulus interval while their behaviour was monitored at 500 fps. We also provided 250 ms trains of light pulses at 20 or 40 Hz. (B) Opsin expression in spinal motor neurons in a *Tg(mnx1:GAL4;UAS:CoChR-tdTomato)* larva at 5 dpf. Imaging field of view corresponds to black box in (A). A, anterior; D, dorsal; P, posterior; V, ventral. Scale bar 50 μ m. (C) Swim bouts elicited by a pulse train in *Tg(mnx1:GAL4;UAS:CoChR-tdTomato)* larvae (left). The control, opsin-negative larva (right), does not respond within 148 ms after stimulus onset. (D) Tail tracking, showing optogenetically-evoked swim bouts in a CoChR-expressing larva (bottom three rows) and a visually-evoked swim in a control opsin-negative larva (top). tbf, tail beat frequency. (E) Distribution of response latencies for all tail movements in opsin-expressing (red) and control opsin-negative larvae (grey). Dotted line indicates maximum latency (50 ms) for a response to be considered optogenetically-triggered. Control larvae exclusively show long latency responses. Each time bin corresponds to 25 ms. (F,L) Response probability of larvae expressing different opsins for single-pulse (F) or pulse-train (L) stimulation (mean \pm SEM, across fish). G–Q Latency (G,M), bout duration (H,N), tail angle of the first half beat (θ_1 ; I,O), number of cycles (J,P) and tail beat frequency (K,Q) for single-pulse (G–K) or pulse-train (M–Q) stimulation (mean \pm SEM, across fish). See also **Figure 3—figure supplement 1** and **Figure 3—videos 1** and **2**.

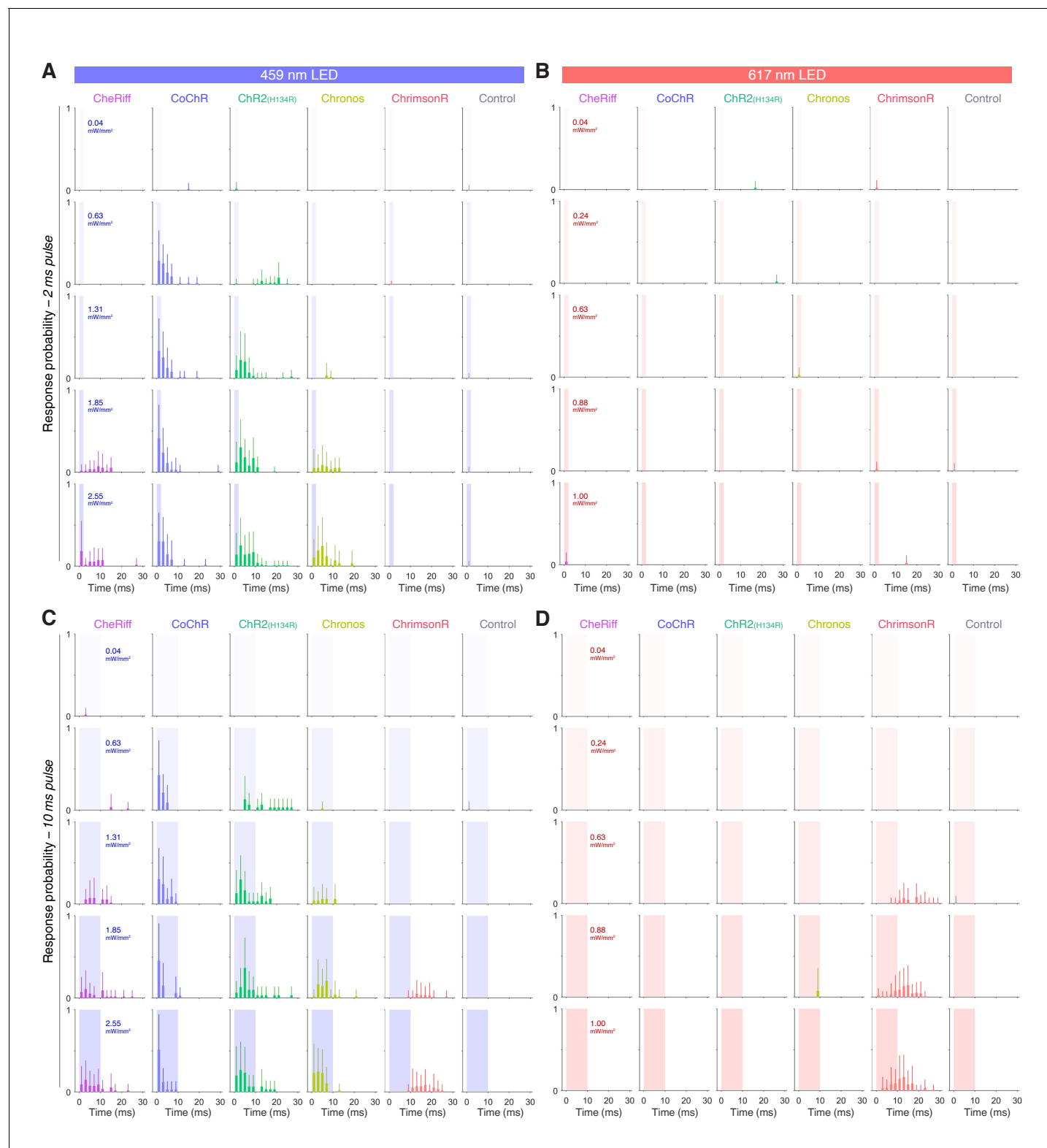


Figure 3—figure supplement 1. Response probability vs. time in larvae expressing opsins in spinal motor neurons. (A–D) Distribution of response probability vs. time for *Tg(mnx1:GAL4)* larvae (6 dpf) expressing different opsins (mean + SD, across fish). Larvae were stimulated with single 2 ms (A,B) or 10 ms (C,D) pulses of blue (459 nm; A,C) or red (617 nm; B,D) light. Each time bin corresponds to 2 ms.

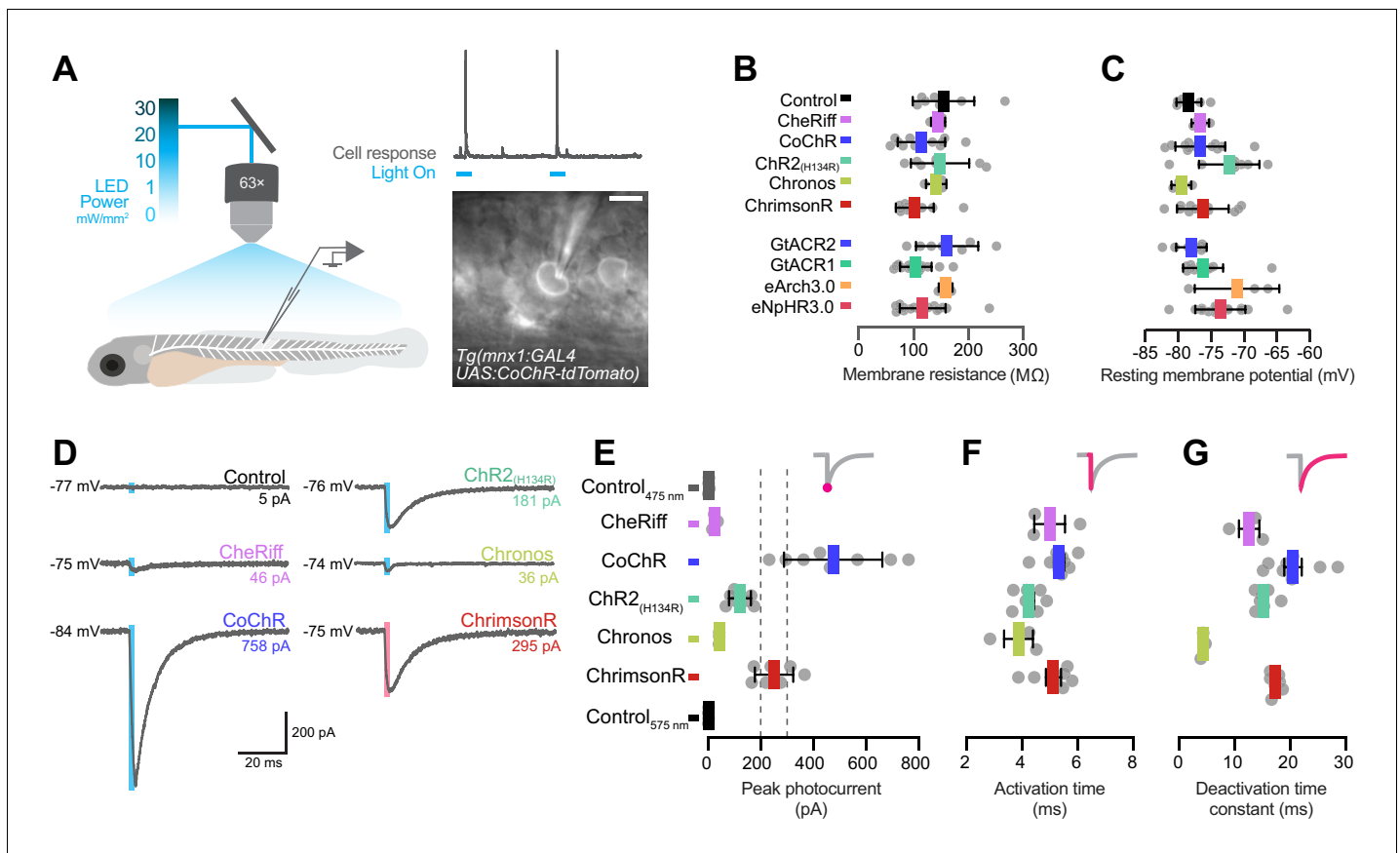


Figure 4. Electrophysiological recording of photocurrents in primary motor neurons. **(A)** Schematics of experimental setup for optogenetic stimulation with in vivo whole-cell patch clamp recordings. Image shows a patched primary motor neuron (pMN) expressing CoChR in a 6 dpf *Tg(mnx1:GAL4;UAS:CoChR-tdTomato)* larva. Scale bar 5 μm . **(B)** Membrane resistance was not affected by opsin expression (mean \pm SD, across cells). **(C)** Resting membrane potential was similar between opsin-expressing and control neurons (mean \pm SD). **(D)** Examples of inward photocurrents in response to 5 ms light pulses (20 mW/mm^2). **(E)** Peak photocurrent amplitude. CoChR and ChrimsonR induced the largest photocurrents (mean \pm SEM, across cells). Dotted lines show range of pMN rheobase. Data is pooled across stimulus intensity (1–30 mW/mm^2) but see **Figure 4—figure supplement 1** for currents at varying irradiance. **(F)** Photocurrent activation time was similar across opsins (mean \pm SEM). **(G)** Chronos photocurrents had the fastest deactivation time constant, while CoChR and ChrimsonR showed similar deactivation kinetics (mean \pm SEM). See also **Figure 4—figure supplement 1**.

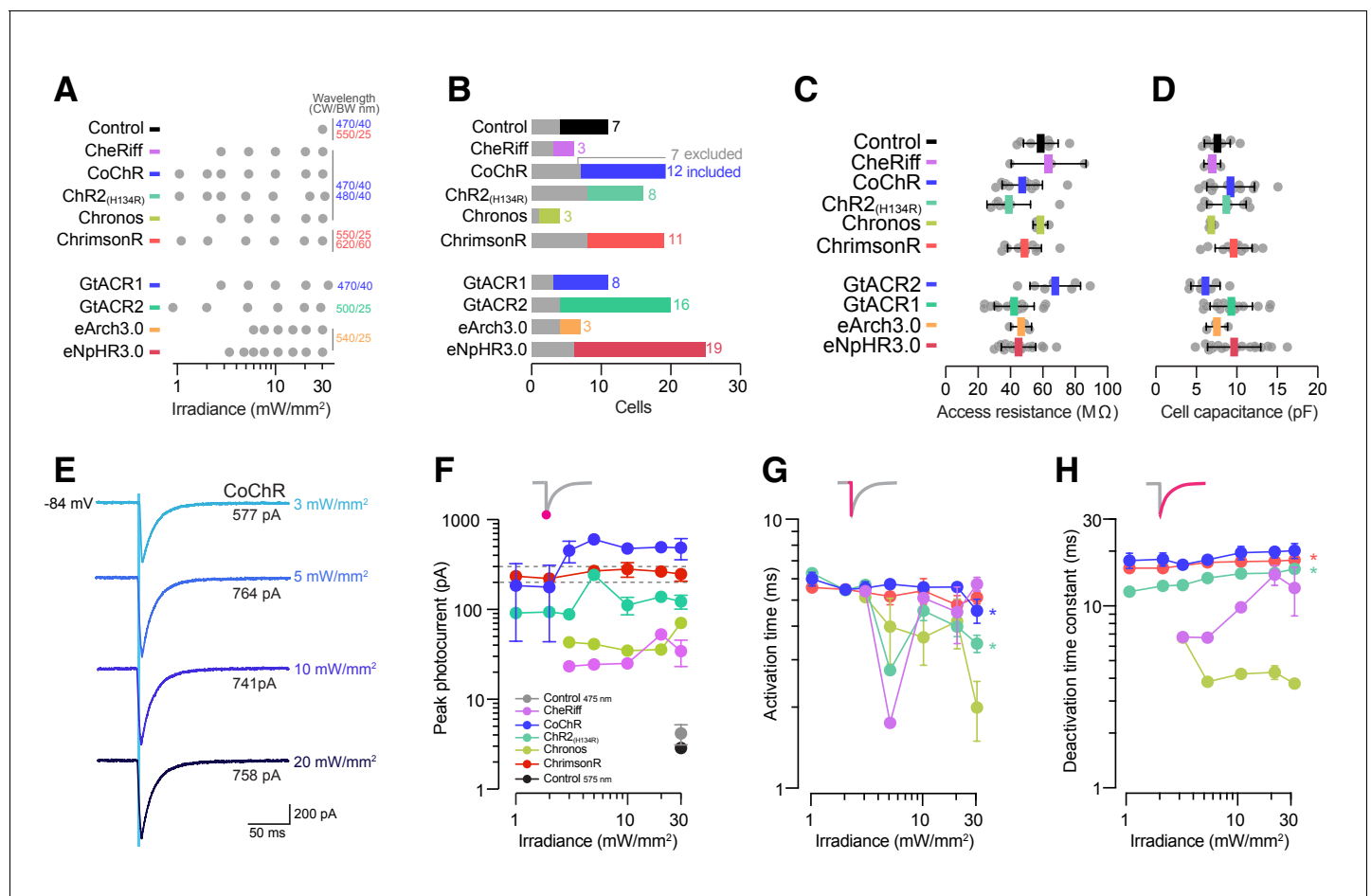


Figure 4—figure supplement 1. Wavelengths used in electrophysiological recordings and photocurrent amplitude and kinetics as a function of irradiance. (A) LED emission wavelength (centre/bandwidth, nm) and irradiance levels used for each opsin line and control cells. (B) Number of cells patched in each group. Numbers and coloured bars indicate included cells while grey bars indicate excluded cells (see Materials and methods for inclusion criteria). (C,D) Access resistance (C) and cell capacitance (D) were comparable between groups (mean \pm SD, across cells). (E) Example photocurrents from a CoChR-expressing cell at different irradiances (3–20 mW/mm²). F–H Peak photocurrent amplitude (F), activation time (G) and deactivation time constant (H) vs. irradiance (mean \pm SEM, across cells). Dotted lines in (F) show range of pMN rheobase. Asterisks indicate a significant non-zero slope.

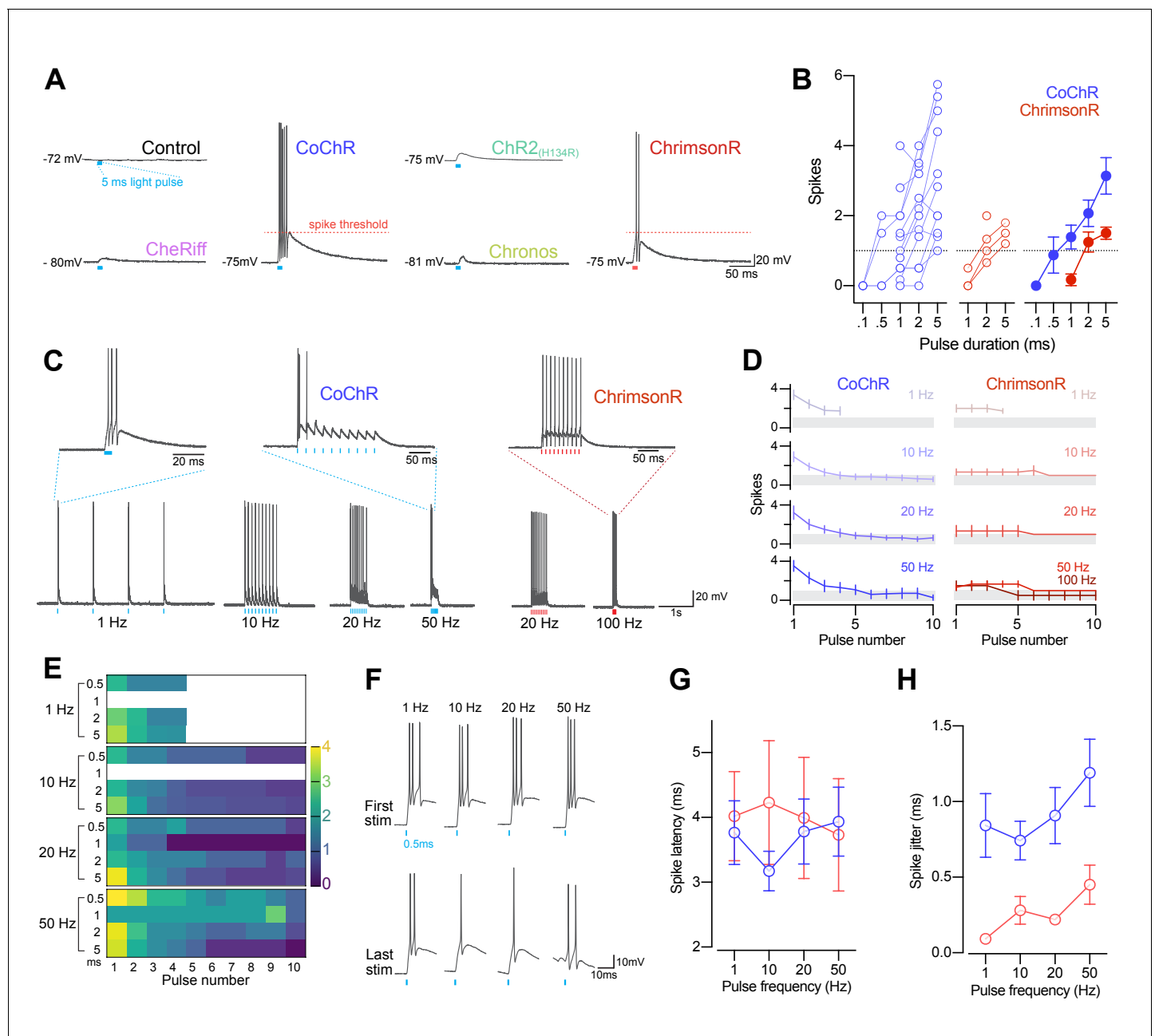


Figure 5. CoChR and ChrimsonR can elicit spiking in primary motor neurons. **(A)** Example membrane depolarisations induced by 5 ms light pulses (20 mW/mm²). **(B)** Number of optogenetically-evoked spikes vs. pulse duration (across irradiance levels 1–30 mW/mm²). Longer pulse duration induced more spikes in both CoChR- and ChrimsonR-expressing cells. Left plots show single neurons and right plot shows mean \pm SEM across cells. **(C)** Example voltage responses from CoChR- and ChrimsonR-expressing cells upon pulse train stimulation (1–100 Hz, 2–5 ms pulse duration). **(D)** Number of spikes vs. pulse number within a train (mean \pm SEM, across cells; shaded area depicts average number of spikes is below 1). In CoChR-expressing cells, the initial 3–4 pulses within the train induced bursts of 2–4 spikes. **(E)** Heatmap of mean spike number elicited via CoChR stimulation, separated according to stimulation frequency and pulse duration. Primary motor neurons often responded with bursts of action potentials, even for short light pulses. **(F)** Example responses to the 1st (top) and last (bottom) 0.5 ms light pulse in a train, recorded from a CoChR-positive neuron. **(G)** Spike latency vs. pulse frequency (mean \pm SEM). **(H)** Spike jitter (mean \pm SEM) vs. pulse frequency shows that ChrimsonR-expressing cells exhibited lower spike jitter than CoChR-expressing cells. See also **Figure 5—figure supplement 1**.

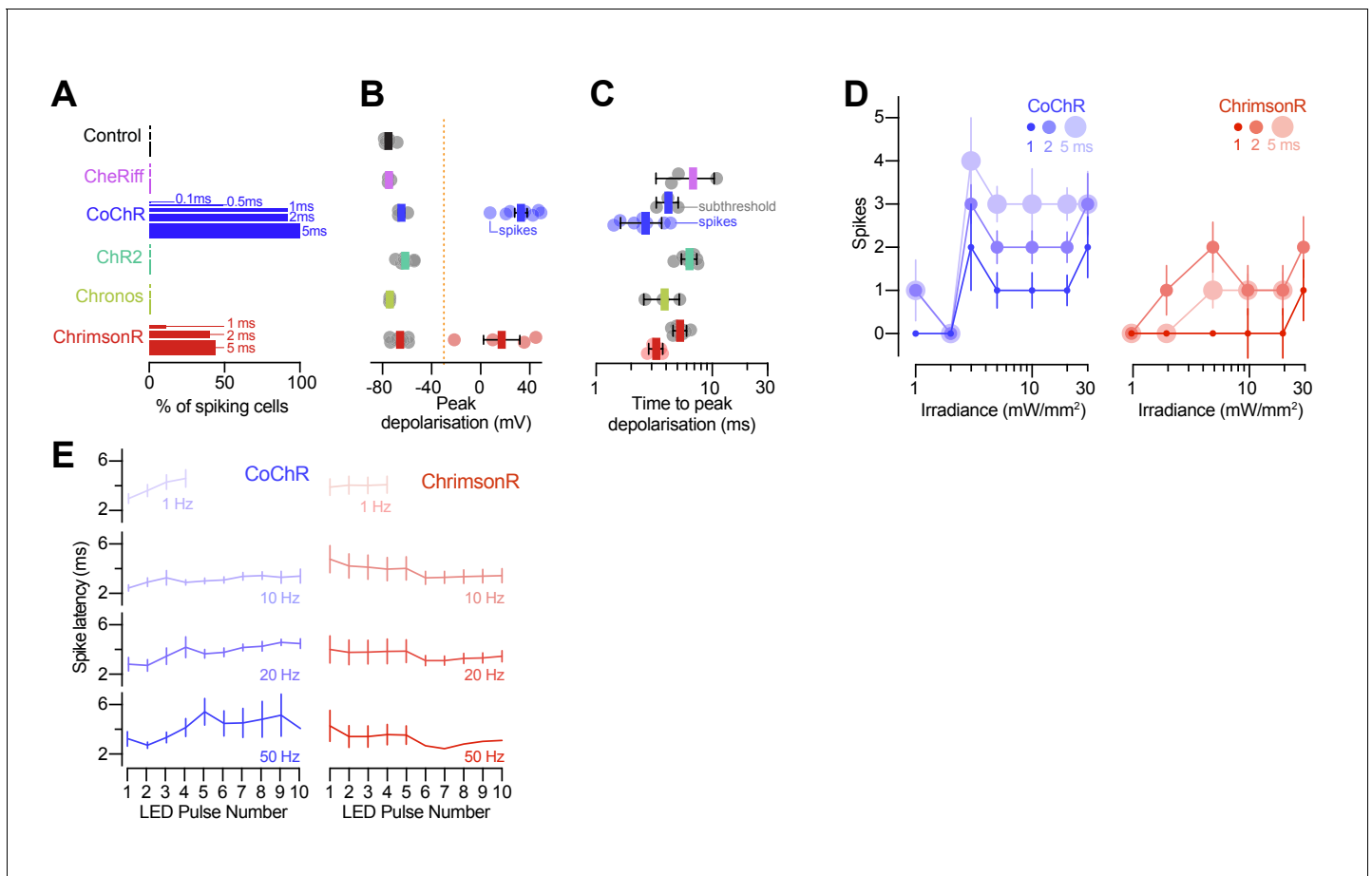


Figure 5—figure supplement 1. Optogenetically-evoked voltage responses as a function of irradiance and pulse frequency. (A) Fraction of cells that generated spikes in response to single light pulses (0.1–5 ms). (B) Peak depolarisation across irradiance levels (1–30 mW/mm²; mean ± SEM, across cells). Orange line indicates threshold for spike detection (–30 mV). (C) Time to peak depolarisation (mean ± SEM). (D) Number of evoked spikes vs. irradiance (1–5 ms pulse duration). In CoChR-expressing cells, 2–5 ms light pulses induced spike bursts (mean ± SEM). (E) Spike latency vs. pulse number (mean ± SEM). With increasing pulse frequency, CoChR-expressing cells showed progressively longer spike latency throughout the pulse train.

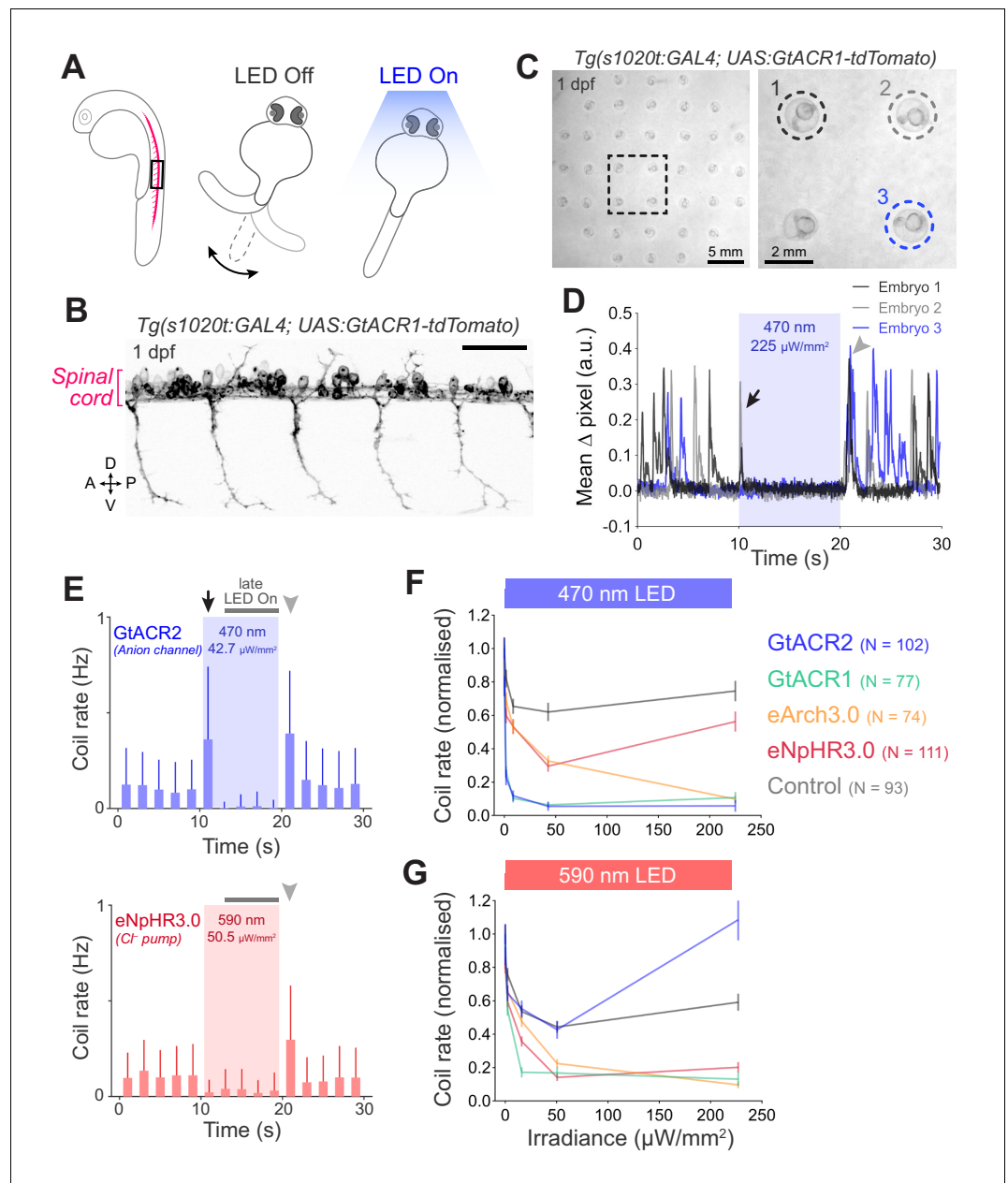


Figure 6. Optogenetic suppression of coiling behaviour in embryos. (A) Schematic of the behavioural assay. (B) Opsin expression in spinal motor neurons and interneurons in a *Tg(s1020t:GAL4; UAS:GtACR1-tdTomato)* embryo at 1 dpf. Imaging field of view corresponds to black box in (A). A, anterior; D, dorsal; P, posterior; V, ventral. Scale bar 50 μm . (C) Camera field of view showing *Tg(s1020t:GAL4; UAS:GtACR1-tdTomato)* embryos positioned in individual agarose wells. Behaviour was monitored at 50 frames per second across multiple embryos (24–27 hpf; $N = 91 \pm 16$ fish per group, mean \pm SD) subjected to 10 s light periods (470 or 590 nm, 0–227 $\mu\text{W}/\text{mm}^2$) with a 50 s inter-stimulus interval. (D) Tracking of coiling behaviour (mean Δ Pixel from three trials) for the three embryos shown in (C). Black arrow indicates movements at light onset, whereas grey arrowhead indicates synchronised restart of coiling behaviour following light offset. (E) Optogenetically-induced changes in coil rate (mean \pm SD, across fish) in embryos expressing the anion channelrhodopsin GtACR1 (N = 77 embryos, top) or the Cl^- pump eNpHR3.0 (N = 111 embryos, bottom). Horizontal dark grey bars indicate the 'late LED On' period. Each time bin corresponds to 2 s. (F, G) Normalised coil rate during the 'late LED On' period in embryos expressing different opsins (mean \pm SEM, across fish). Control opsin-negative siblings were subjected to the same light stimuli. See also **Figure 6—figure supplements 1 and 2** and **Figure 6—video 1**.

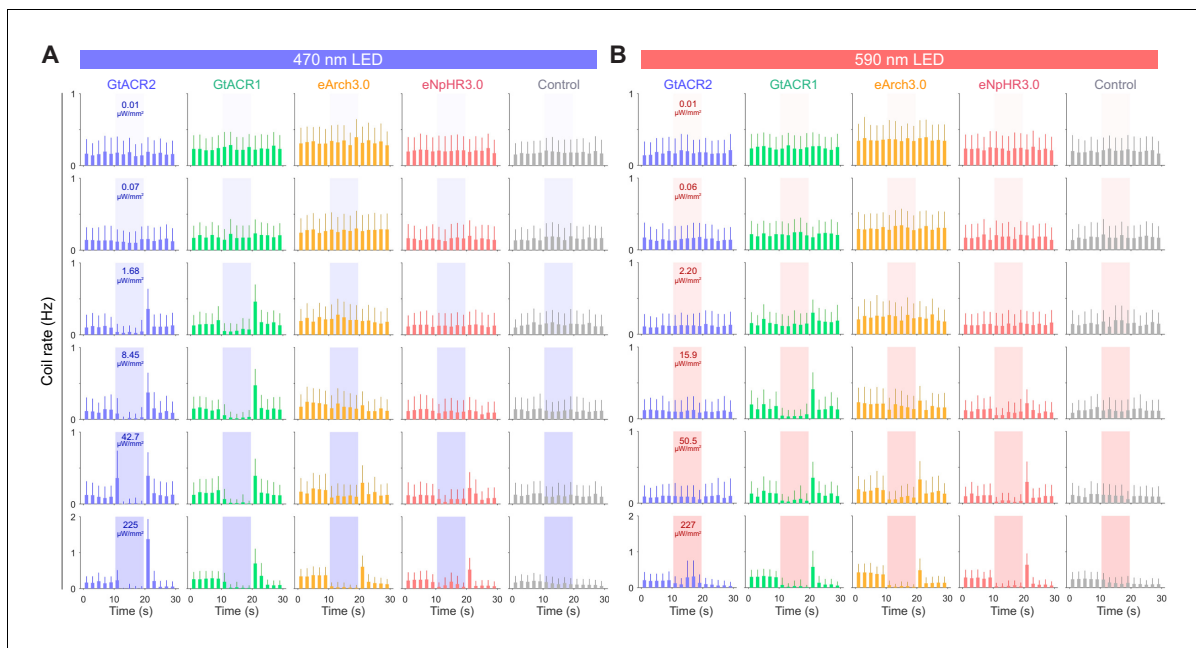


Figure 6—figure supplement 1. Coil rate vs. time in embryos expressing different opsins in spinal neurons. (A,B) Distribution of coil rate vs. time for *Tg(s1020t:GAL4)* embryos (24–27 hpf) expressing different opsins (mean + SD, across fish). Embryos were subjected to 10 s pulses of blue (470 nm; A) or amber (590 nm; B) light. Each time bin corresponds to 2 s.

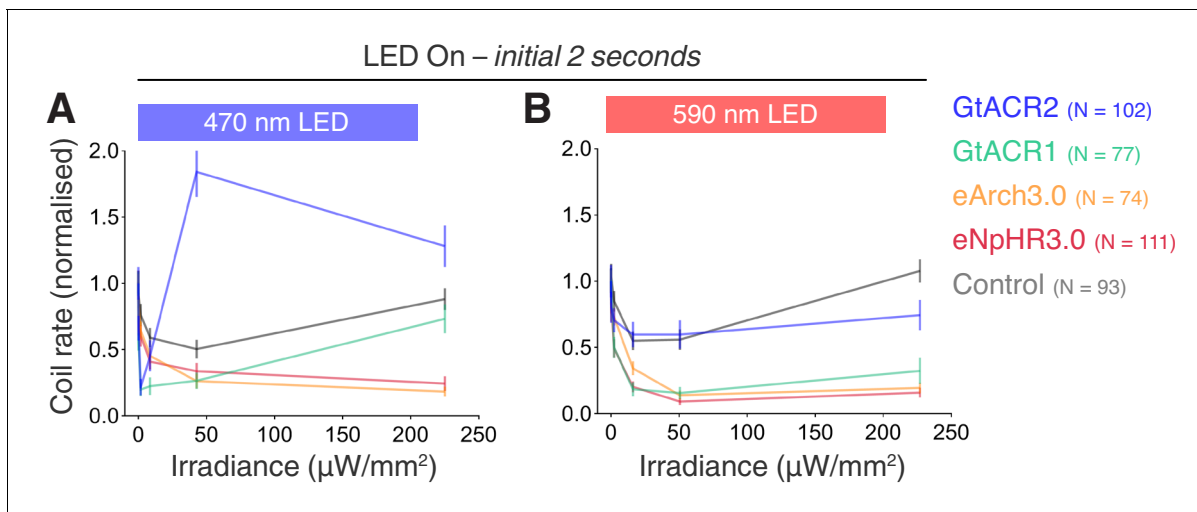


Figure 6—figure supplement 2. Coil rate vs. irradiance for the initial 2 s of light exposure. (A,B) Normalised coil rate during the initial 2 s of the LED On period in embryos (24–27 hpf) expressing different opsins (mean \pm SEM, across fish). Control opsin-negative siblings were subjected to the same light stimuli.

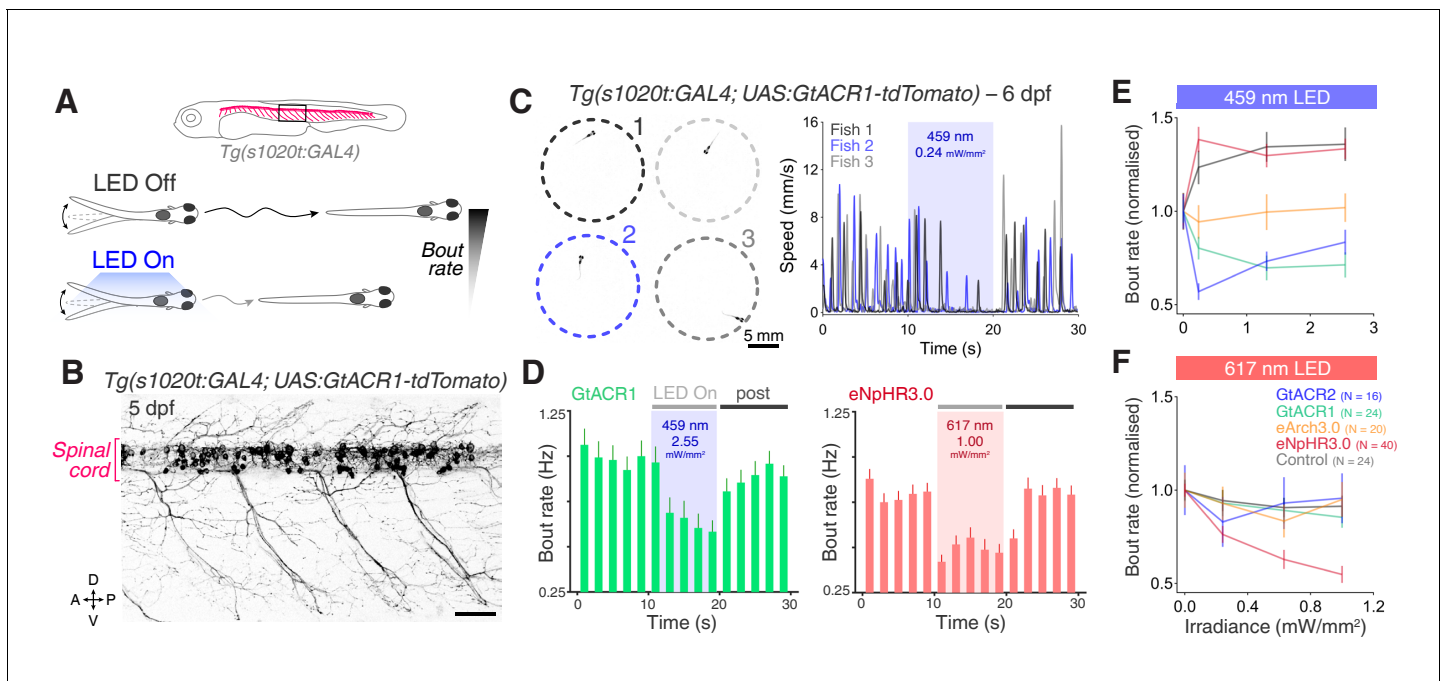


Figure 7. Optogenetic suppression of swimming in larvae. (A) Schematic of behavioural assay. (B) Opsin expression in spinal motor neurons and interneurons in a *Tg(s1020t:GAL4;UAS:GtACR1-tdTomato)* larva at 5 dpf. Imaging field of view corresponds to black box in (A). A, anterior; D, dorsal; P, posterior; V, ventral. Scale bar 50 μm . (C) *Tg(s1020t:GAL4;UAS:GtACR1-tdTomato)* larvae were positioned in individual agarose wells (left) and instantaneous swim speed was monitored by centroid tracking (right) at 50 fps (six dpf; N = 25 \pm 9 fish per group, mean \pm SD). 10 s light periods were delivered (459 or 617 nm, 0–2.55 mW/mm²) with a 50 s inter-stimulus interval. (D) Optogenetically-induced changes in bout rate (mean \pm SEM, across fish) in *Tg(s1020t:GAL4)* larvae expressing *GtACR1* (N = 24 larvae, left) or *eNpHR3.0* (N = 40 larvae, right). Horizontal grey bars indicate the time windows used to quantify behavioural changes. Each time bin corresponds to 2 s. (E,F) Normalised bout rate during the ‘LED On’ period in larvae expressing different opsins (mean \pm SEM, across fish) and in control, opsin-negative, siblings. See also **Figure 7—figure supplements 1–4** and **Figure 7—video 1**.

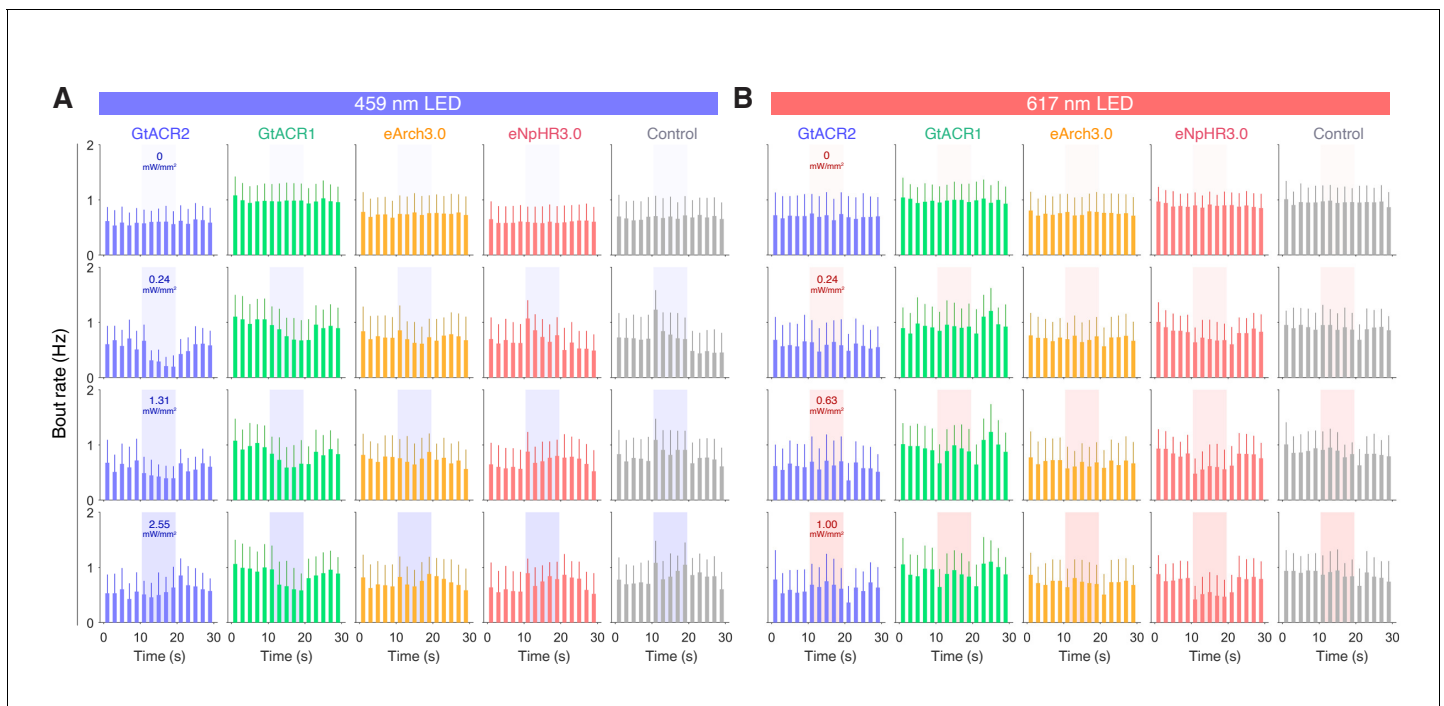


Figure 7—figure supplement 1. Bout rate vs. time in larvae expressing different opsins in spinal neurons. (A,B) Distribution of bout rate vs. time for *Tg* (*s1020t:GAL4*) larvae (6 dpf) expressing different opsins (mean + SD, across fish). Larvae were subjected to 10 s pulses of blue (459 nm; A) or red (617 nm; B) light. Each time bin corresponds to 2 s.

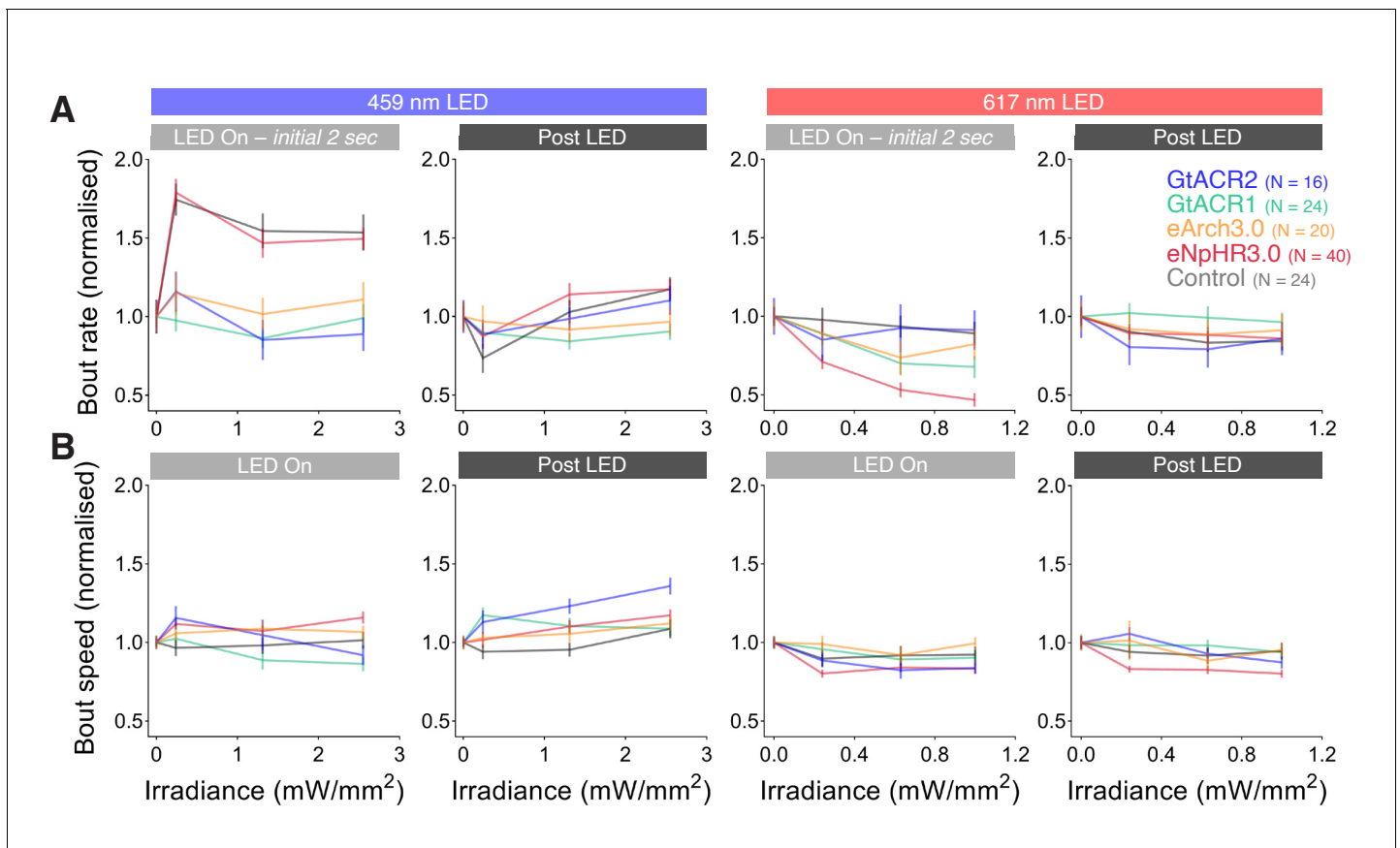


Figure 7—figure supplement 2. Bout rate and speed vs. irradiance during different time periods in *Tg(s1020t:GAL4)* larvae. (A,B) Normalised bout rate (A) or bout speed (B) during the whole LED On period, the initial 2 s of light exposure and the ‘post LED’ 8 s period in *Tg(s1020t:GAL4)* larvae (6 dpf) expressing different opsins (mean \pm SEM, across fish). Control opsin-negative siblings were subjected to the same light stimuli.

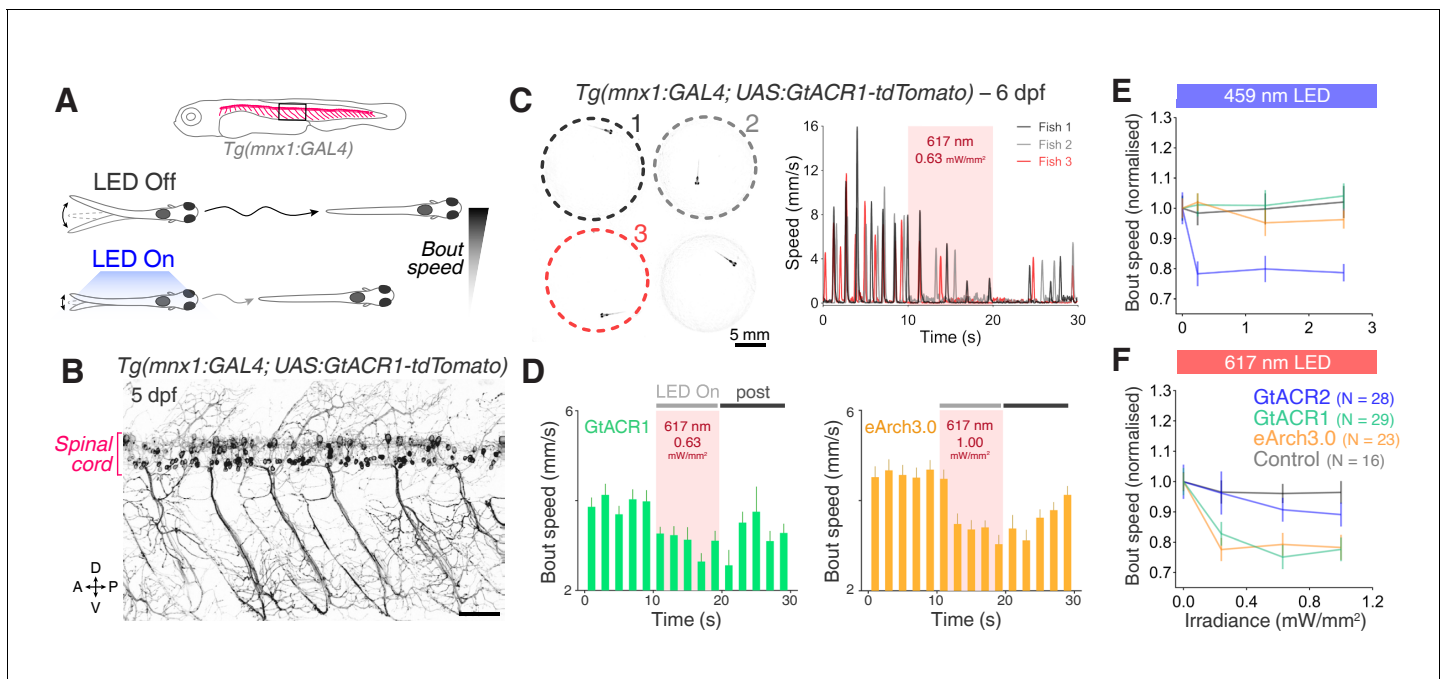


Figure 7—figure supplement 3. Optogenetic suppression of swimming in *Tg(mnx1:GAL4)* larvae. **(A)** Schematics of opsin expression pattern and behavioural assay. **(B)** Opsin expression in spinal motor neurons in a *Tg(mnx1:GAL4;UAS:GtACR1-tdTomato)* larva at 5 dpf. Imaging field of view corresponds to black box in **(A)**. A, anterior; D, dorsal; P, posterior; V, ventral. Scale bar 50 μm . **(C)** Background-subtracted camera field of view showing *Tg(mnx1:GAL4;UAS:GtACR1-tdTomato)* larvae positioned in individual agarose wells (left) and tracking of swimming speed for selected larvae (right). Behaviour was monitored at 50 fps across multiple freely-swimming larvae (6 dpf; $N = 24 \pm 6$ fish per group, mean \pm SD) while they were subjected to 10 s light periods (459 or 617 nm, 0–2.55 mW/mm²) with a 50 s inter-stimulus interval. **(D)** Optogenetically-induced changes in bout rate (mean \pm SEM, across fish) in *Tg(mnx1:GAL4)* larvae expressing *GtACR1* ($N = 29$ larvae, left) or *eArch3.0* ($N = 23$ larvae, right). Horizontal grey bars indicate the time windows used for comparative quantification of behavioural changes. Each time bin corresponds to 2 s. **(E,F)** Normalised bout speed during the ‘LED On’ period in larvae expressing different opsins (mean \pm SEM, across fish). Control opsin-negative siblings were subjected to the same light stimuli.

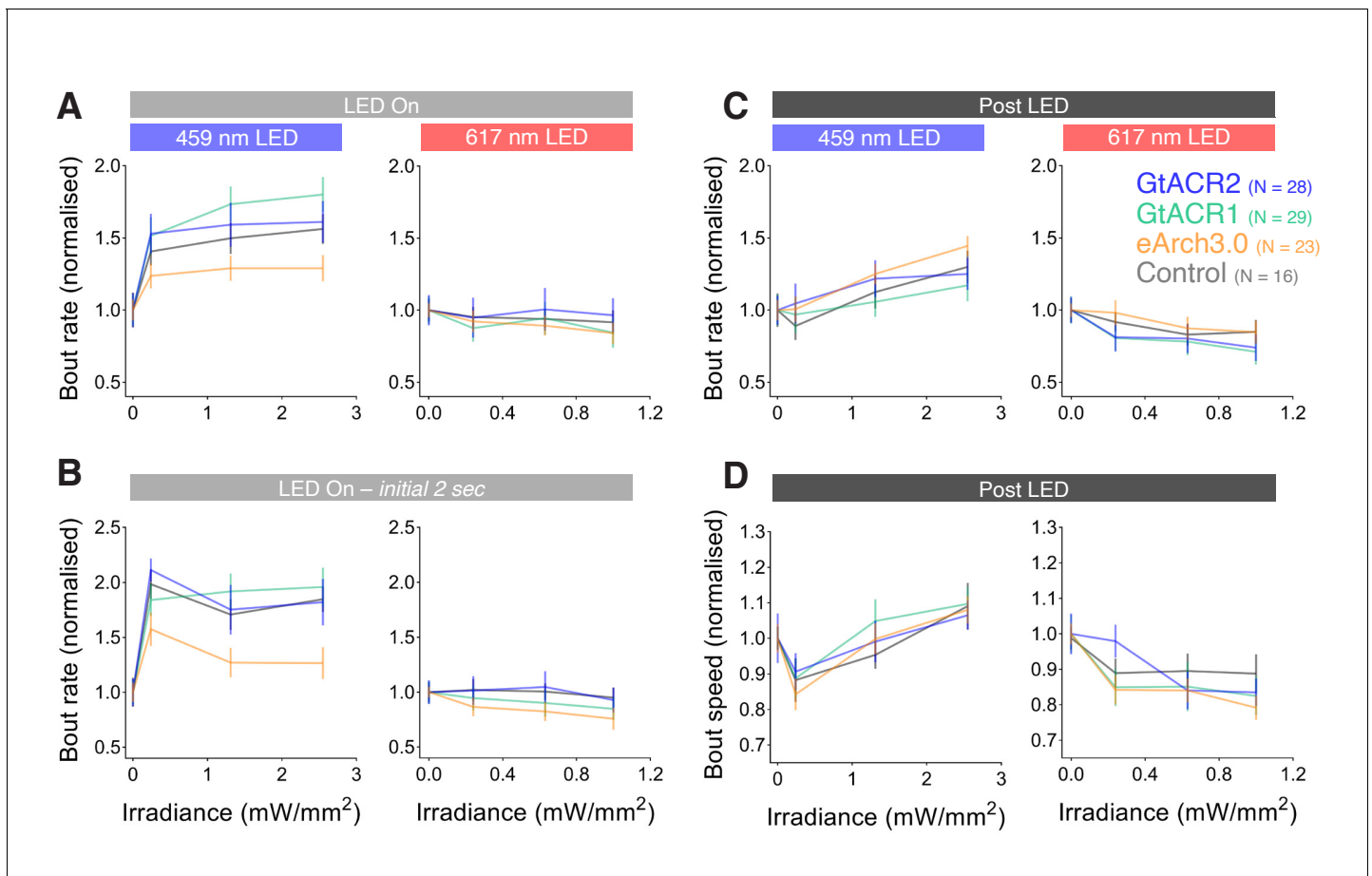


Figure 7—figure supplement 4. Bout rate and speed vs. irradiance during different time periods in *Tg(mnx1:GAL4)* larvae. (A–D) Normalised bout rate (A–C) or bout speed (D) during the whole ‘LED On’ period (A), the initial 2 s of the light period (B), or the ‘post LED’ 8 s period (C,D) in *Tg(mnx1:GAL4)* larvae (6 dpf) expressing different opsins (mean ± SEM, across fish). Control opsin-negative siblings were subjected to the same light stimuli.

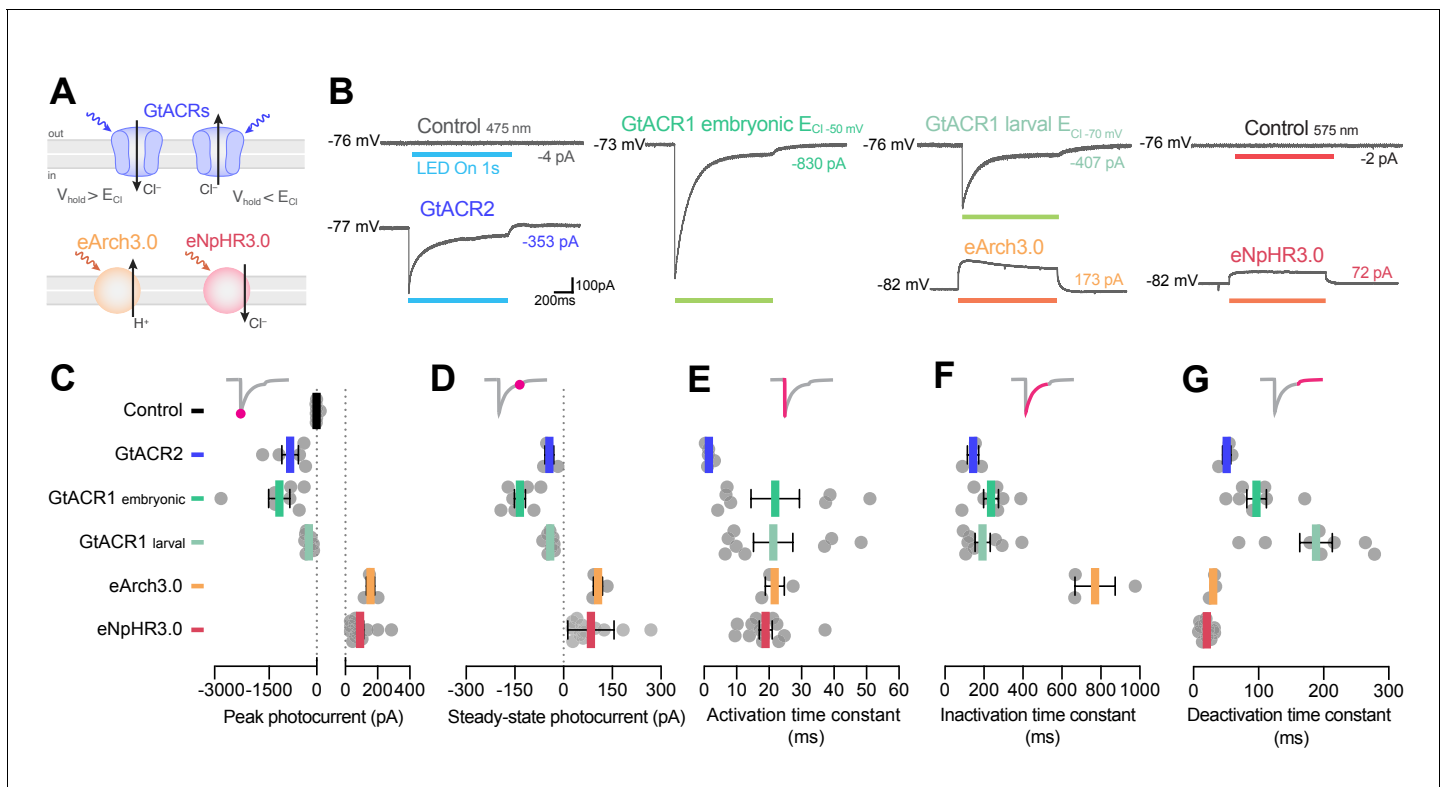


Figure 8. Photocurrents induced by anion channelrhodopsins and chloride/proton pumps. (A) Action of anion channelrhodopsins (top) and Cl^-/H^+ pumps (bottom). For anion channelrhodopsins, photocurrent magnitude and direction depend on chloride reversal potential (E_{Cl}) and holding potential (V_{hold}), while Cl^-/H^+ pumps always induce outward currents. (B) Example photocurrents in response to a 1 s light exposure (20 mW/mm²). (C, D) Photocurrent peak (C) and steady-state (D) amplitude (mean \pm SEM, across cells). GtACRs induced larger photocurrents than Cl^-/H^+ pumps. (E–G) Photocurrent activation (E), inactivation (F) and deactivation (G) time constants (mean \pm SEM). Photocurrents induced by Cl^-/H^+ pumps showed minimal inactivation and faster deactivation kinetics than GtACRs. eNpHR3.0 photocurrents did not inactivate hence no inactivation time constant was computed. See also **Figure 8—figure supplement 1**.

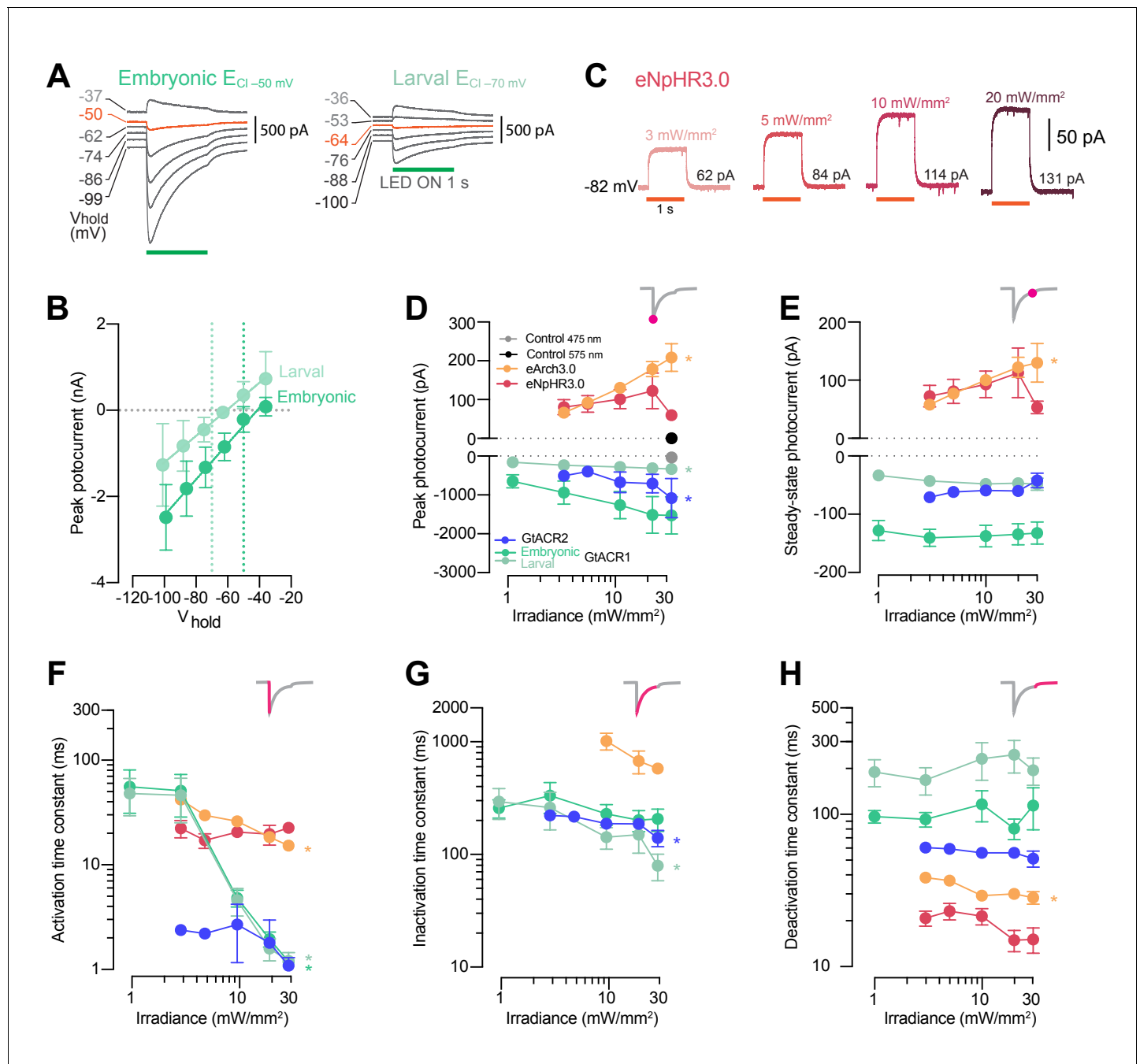


Figure 8—figure supplement 1. Photocurrent amplitude and kinetics as a function of irradiance. (A) Example GtACR1 photocurrents obtained by providing a 1 s light period at different holding potentials (V_{hold}) using intracellular solutions approximating either embryonic or larval E_{Cl} . Orange traces denote holding potentials closest to E_{Cl} . (B) GtACR1 photocurrent I-V curves (mean \pm SD). Photocurrents reverse with a positive 5–10 mV shift relative to E_{Cl} (dotted lines) in both solutions. (C) Example photocurrents from an eNpHR3.0-expressing cell at different irradiance levels (3–20 mW/mm²). (D,E) Photocurrent peak (D) and steady-state (E) amplitude vs. irradiance (mean \pm SEM, across cells). Asterisks indicate a significant non-zero slope. F–H Photocurrent activation (F), inactivation (G) and deactivation (H) time constants vs. irradiance (mean \pm SEM). eNpHR3.0 photocurrents did not inactivate hence no inactivation time constant was computed.

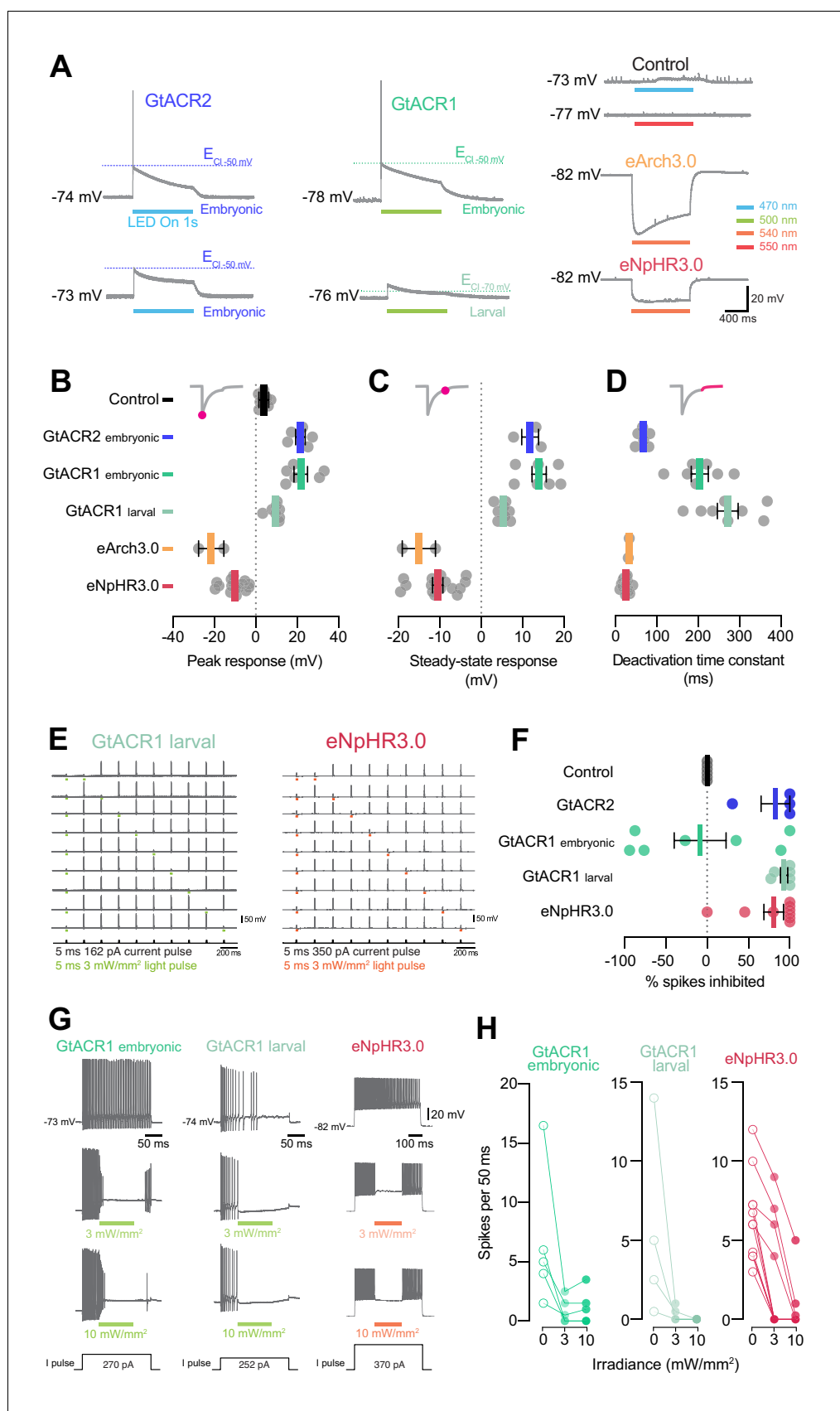


Figure 9. GtACRs and eNpHR3.0 effectively inhibited spiking. (A) Example voltage deflections induced by anion channelrhodopsins and Cl^-/H^+ pumps in response to a 1 s light pulse (20 mW/mm^2). (B–D) Peak (B) and steady-state (C) responses and deactivation time constant (D) of voltage deflections. All opsins induced similar absolute voltage changes. Anion channelrhodopsins generated depolarisation with both intracellular solutions while Cl^-/H^+ pumps generated hyperpolarisation. (E) Example recordings demonstrating inhibition of single spikes in GtACR1- and eNpHR3.0-expressing cells with 5 ms light pulses (3 mW/mm^2). (F) Fraction of spikes that were optogenetically inhibited (mean \pm SEM, across cells). All opsins achieved high suppression efficacy, but GtACR1 induced additional spikes upon light delivery with the embryonic intracellular solution. (G) Example recordings demonstrating inhibition of sustained spiking in GtACR1- and eNpHR3.0-expressing cells. (H) Quantification of suppression using protocol illustrated in (G). Number of spikes per 50 ms during light delivery ($0\text{--}10 \text{ mW/mm}^2$) is plotted against irradiance. GtACR1 and eNpHR3.0 inhibited tonic spiking with similar efficacy (mean \pm SEM). See also **Figure 9—figure supplement 1**.

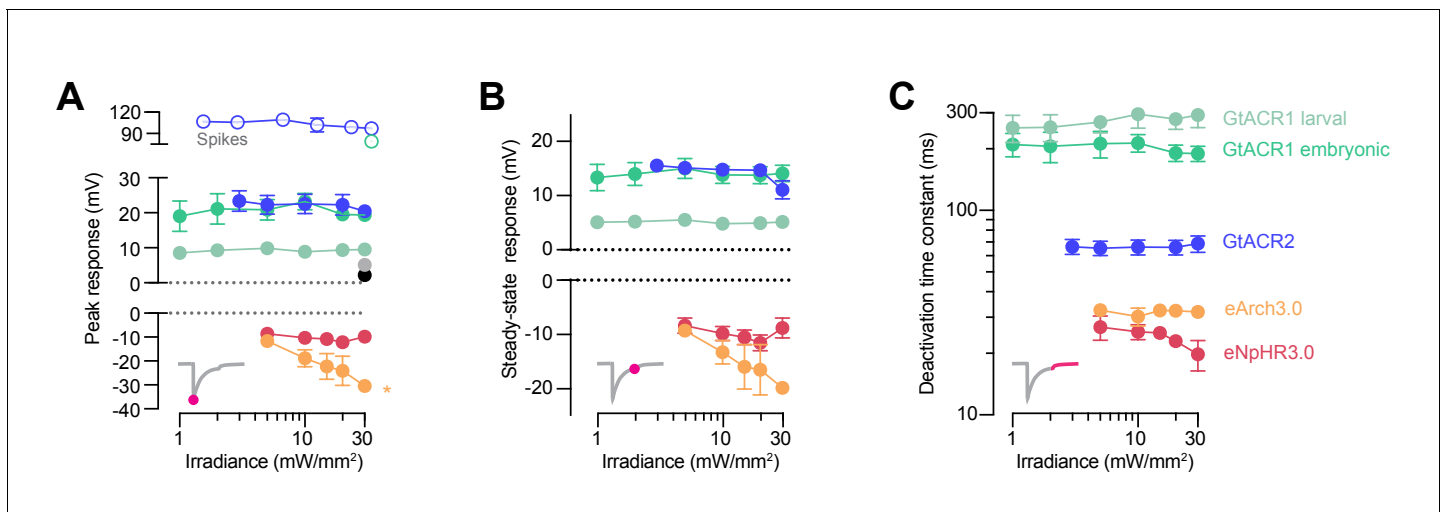


Figure 9—figure supplement 1. Optogenetically-evoked voltage responses as a function of irradiance. (A–C) Peak (A) and steady-state (B) responses and deactivation time constant (C) of voltage deflections vs. irradiance (mean \pm SEM, across cells). eArch3.0 was the only opsin showing irradiance-dependent modulation of peak voltage response.

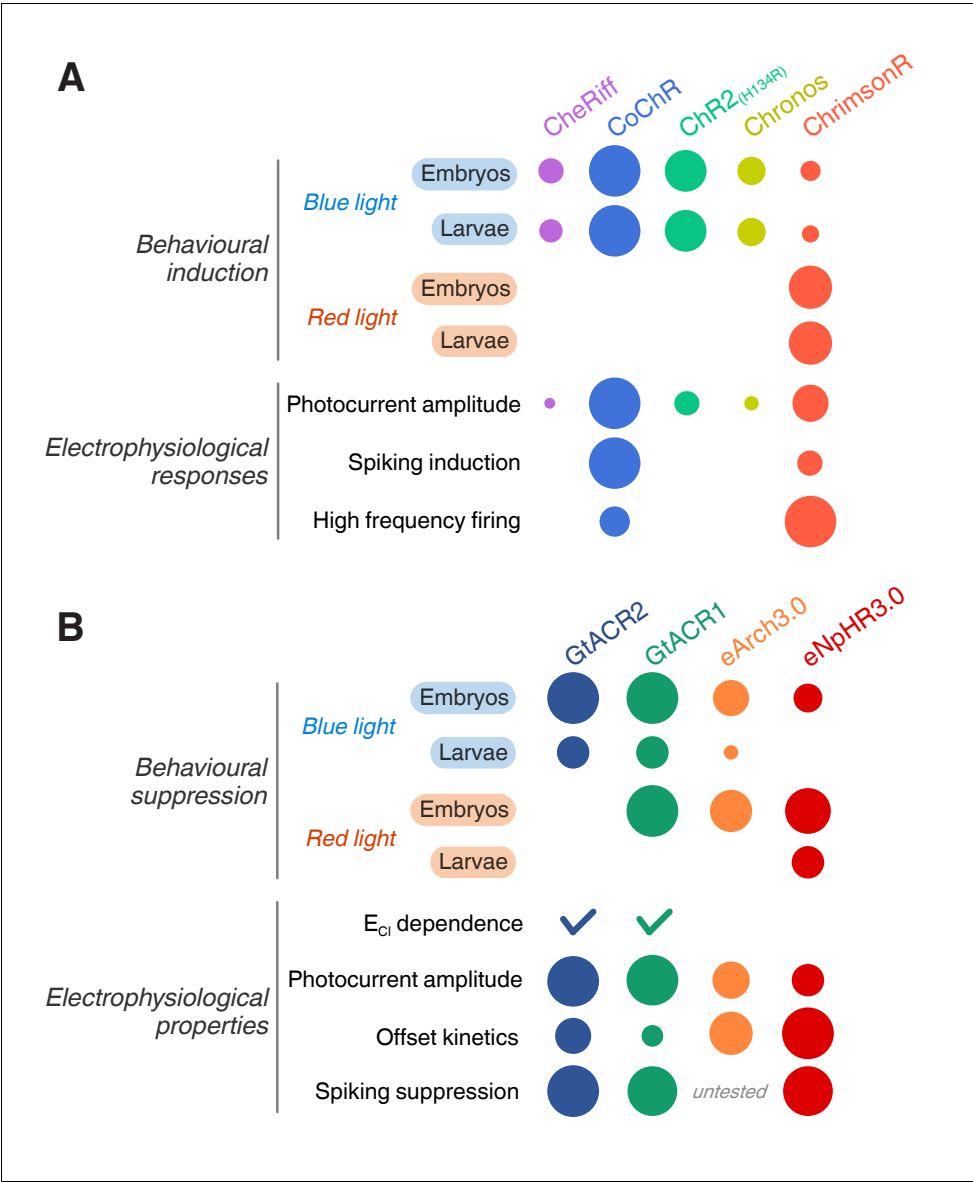


Figure 10. Summary of opsin line efficacy. (A) Efficacy of cation channelrhodopsin lines in inducing neural activity across behavioural assays, electrophysiological recordings, developmental stages and wavelengths. The radius of each circle is proportional to efficacy. (B) Efficacy of anion channelrhodopsins and Cl⁻/H⁺ pumps in suppressing neural activity.